Journal of Mines, Metals and Fuels, *71(12C) : 453-361; 2023. DOI: 10.18311/jmmf/2023/47296*

Print ISSN : 0022-2755

Journal of Mines, Metals and Fuels

Contents available at: *www.informaticsjournals.com/index.php/jmmf*

Combined Effect of Viscous Dissipation and Forchheimer Drag on 3D Nanofluid Flow over Non-linear Stretching Sheet

K. N. Manoharkumar[1*], Shalini M. Patil[2], P. A. Dinesh[3], K. V. Suma[4], C. V. Vinay[2] and Chitirala Subrahmanyam[5]

[1]Department of Mathematics, K S School of Engineering and Management (Affiliated to Visvesvaraya Technological University), Bengaluru – 560109, Karnataka, India; manoharknkumar@gmail.com

[2]Department of Mathematics, JSS Academy of Technical Education, Bengaluru – 560060, Karnataka, India; patilshalini75@gmail.com, vinaycv@jssateb.ac.in

[3]Department of Mathematics, M S Ramaiah Institute of Technology, Bengaluru – 560054, Karnataka, India; dineshdpa@msrit.edu

[4]Department of Electronics and Communication Engineering, M S Ramaiah Institute of Technology, Bengaluru – 560054, Karnataka, India

[5]Department of Mathematics, New Horizon College of Engineering, Bengaluru – 560087, Karnataka, India; manyamchs@gmail.com

Abstract

Present study investigates the impact of viscous dissipation and drag force on 3D – Darcy Forchheimer nanofluid flow over flat surface induced by bi-directional power law stretching sheet. Inflated flow rate in the considered region is encountered by velocity square in the momentum equation. The principal model is represented as highly nonlinear homogenous ODE. By using suitable similarity transformation PDE is modified into dimensionless ODE which is then tackled by RKF-NR approach. The computational results are depicted through graphical representation on velocity, temperature and concentration for various range of nondimensional physical components such as Schmidt, Eckert, Prandtl and Forchheimer numbers. Outcomes of the current findings has found various applications in industry viz solar energy, crystal growth and metal working processes. Results are in good agreement upon comparing with the earlier studies.

Keywords: *Boundary Layer, Forchheimer, Nanofluid, Non-Linear Stretching Sheet, Viscous Dissipation*

1.0 Introduction

Three-dimensional fluid flow refers to the movement of fluid in a three-dimensional space, considering variations not only in length and width but also in depth. This type of flow is prevalent in many natural and engineered systems *viz*., ocean currents, atmospheric circulation to industrial processes and biological systems. Understanding three-dimensional fluid flow is crucial for various applications, including designing efficient aircraft and ships, optimizing chemical processes, and predicting weather patterns. However, it poses significant challenges due to the complex interactions between different fluid layers and the effects of turbulence. Studying 3D fluid movement over a

**Author for correspondence*

nonlinear extending sheet provides valuable insights into fundamental fluid mechanics principles and practical engineering applications. It aids in the development of predictive models, optimization strategies, and the design of innovative technologies aimed at improving efficiency and performance in various industrial processes.

Masood *et al.,*[1] studied the Cattaneo-Christov model and the behaviour of a viscous fluid comprising nanoparticles on an elastic surface while considering thermophoresis and Brownian motion. In understanding the applications pertaining to medical treatments of cancer, tumor, x-ray and plastic thin films a numerical study is developed to know the variations of Darcy-Forchheimer relation over non-linear stretching sheet under convective MHD nanofluid flow studied by Rasool *et al.,*[2]. To study the applications in lubrication and petroleum industry Aissa Abderrahmane *et al.,*[3] analysed the heat transport properties of a non-Newtonian hybrid nanofluid consisting of carboxy-methyl-cellulose and aluminium oxide by considering Darcy – Brinkman model and investigated the transfer of heat inside the porous annulus enclosure, the study is conducted for both convective boundary conditions and magnetohydrodynamics taking into account. Moses Dada and Funmilayo Adefolaju[4] investigated the mass transfer and viscous, incompressible energy properties of a nanofluid flowing across a perpendicular plane while accounting for the loss of heat and heat radiation in the Darcy – Forchheimer porous medium by considering roseland diffusion approximation. Bhatti *et al.,*[5] analysed the effect of bioheat and mass transport on the peristaltic-driven fluid transport in porous medium by taking into account chemical reaction and extrinsic magnetic field. Dinesh *et al.,*[6] worked on thorough examination of the mixed effects of double diffusive mixed heat and mass movement, internal heat production and viscous loss while taking into account the Forchheimer model. Specifically, the investigation considered exponential variations in the fluid properties of solutal dispersion, thermal transfer, porosity, and permeability. Dinesh *et al.,*[7] conducted the numerical analysis of paired heat and mass transmission in heated surface that is slightly angled by using the components porosity, heat conduction and permeability in a thinly packed porous medium in a non-compressible viscous fluid. Bandaru[8] analysed the convective heat movement and mass transmission through rotation of a fluid past an upward sheet placed inside a porous material. A non-Darcy Forchheimer is used to account for inertia impacts and an erratic heat source. Alrihieli *et al.,*[9] described how changing thermo-physical variables influence the movement of a Maxwell MHD nanofluid approaching a flexible symmetrical surface, in addition to the effects of convective heating and viscous dissipation. Sheikholeslami *et al.,*[10] investigated effects of the thermal conductance and stickiness of the nanofluid between the two parallel plane surfaces by considering the heat transmission properties utilizing KKL model.

Metals, mines, and fuels play vital roles in numerous industrial sectors *viz*., mining ventilation systems, hydraulic fracturing in oil and gas extraction, oil and gas pipeline transportation, metal casting and forming processes, fuel injection systems in combustion engines are essential to underpin modern society, driving economic growth, technological innovation, and global development across a diverse range of industries and applications.

Ramesh *et al.,*[11] conducted analytical study on diffusion thermo effect of Casson fluid over mixed convective flow in porous media through inclined channel to apply in various industrial uses *viz*., textile, irrigation, petroleum processing and polymer industries. Kavitha *et al.,*[12] examined the impact of steady and dusty fluids of second order resistance while taking permeability, thermal conductivity, and porosity into account in MHD and will be applied in astrophysics, catalytic reactors, oceanography. Roopa *et al.,*[13] examined the unsteady state of hybrid nanofluid Fe_3O_4 and Graphene by taking water as base fluid in magnetohydrodynamic flow over an extended surface by analysing the properties of heat and Fuchs radiation. Khan *et al.,*[14] examined the bi-directional, nanofluid movement in 3D across non – linearly stretching sheet by taking the variations in the power law index. Raju and Sandeep[15] explored the impacts of nonlinear thermal transport on the multi-dimensional fluid movement across a stretched sheet of Carreau and Casson fluids. Mathematical design of Convective heat transmission of the nanofluid flow is modelled by Buongiorno[16]. Riaz *et al.,*[17] investigated peristaltic motion of nanofluid by utilizing the Jeffrey model on porous rectangular tube for the different wavelength of Reynolds number. Necib *et al.,*[18] conducted numerical analysis to study the fluid movement in saturated porous media and also studied the different kinds of nanofluid particles graphene, TiO_2.

To our knowledge and from the above literature cited, the non-linear effects of viscous dissipation and Forchheimer drag force place a controlling parameter on fluid flow, heat and mass transmission which helps in many cited industrial applications is the main objective of the current work.

In this research, we studied the flow of nanofluids in three dimensions to understand fluid behaviour and transform the governing PDE's into ODE's using similarity transformations along with appropriate boundary conditions. Investigated the effect of non-dimensional variables such as velocity, temperature, and volume fraction profiles through graphical analysis by considering Forchheimer and viscous dissipation effects. Additionally, examined and present skin friction and the decrease in Nusselt number in tabular form.

2.0 Formulation

Consider an incompressible movement of a nanofluid induced owing to surface is extended non-linearly in both the x and y axis (Figure 1). Velocity of the fluid at any point on this surface is described by mathematical expressions involving constants 'a', 'b', and 'n'. By considering effects Forchheimer and viscous dissipation that influence movement of the fluid. The surface is kept at a constant temperature T_w, while the surrounding fluid has a different temperature T_∞. Additionally, we're considering the concentration of particles in the fluid, denoted by C_∞. Analyzing the equations that govern this nonofluid flow in three dimensions, along with the specified boundary conditions can be stated from Khan *et al.*,[14]

$$\frac{\partial u}{\partial x}+\frac{\partial v}{\partial y}+\frac{\partial w}{\partial z}=0, \tag{1}$$

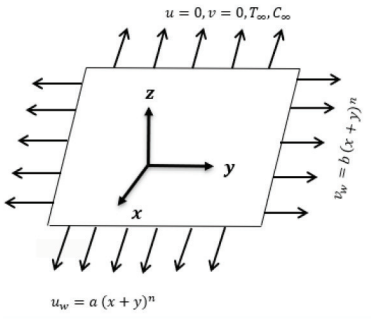


Figure 1. Three-dimensional coordinate system.

$$u\frac{\partial u}{\partial x}+v\frac{\partial u}{\partial y}+w\frac{\partial u}{\partial z}=\nu_f\frac{\partial^2 u}{\partial z^2}+\frac{c_b}{\rho_0\sqrt{k}}u^2, \tag{2}$$

$$u\frac{\partial v}{\partial x}+v\frac{\partial v}{\partial y}+w\frac{\partial v}{\partial z}=\nu_f\frac{\partial^2 v}{\partial z^2}+\frac{c_b}{\rho_0\sqrt{k}}v^2, \tag{3}$$

$$u\frac{\partial T}{\partial x}+v\frac{\partial T}{\partial y}+w\frac{\partial T}{\partial z}=\alpha\frac{\partial^2 T}{\partial z^2} +\tau\left[D_B\frac{\partial C}{\partial z}\frac{\partial T}{\partial z}+\frac{D_T}{T_\infty}\left(\frac{\partial T}{\partial z}\right)^2\right]+\frac{\mu_p}{\rho C_p}\left(\frac{\partial u}{\partial z}\right)^2, \tag{4}$$

$$u\frac{\partial C}{\partial x}+v\frac{\partial C}{\partial y}+w\frac{\partial C}{\partial z}=D_B\frac{\partial^2 C}{\partial z^2}+\frac{D_T}{T_\infty}\frac{\partial^2 T}{\partial z^2}, \tag{5}$$

In this context, we describe the velocity of fluid u, v, and w. represents the fluid's kinematic viscosity, while T denotes the fluid's temperature. D_B stands for the diffusion coefficient of Brownian matter, and D_T represents the parameter for thermophoretic diffusion. α indicates the thermal diffusivity, and τ represents the ratio between the thermal stability of nanoparticles and that of the base fluid.

The given equations define the boundaries

$$u=u_w=a(x+y)^n \ , v=v_w=b(x+y)^n \ ,$$
$$w=0, T=T_w, \quad D_B\frac{\partial C}{\partial z}+\frac{D_T}{T_\infty}\frac{\partial T}{\partial z}=0 \, at \, z=0$$

$$u\to 0, v\to 0, T\to T_\infty, C\to C_\infty \ as \ z\to\infty \tag{6}$$

By utilizing similarity transformations

$$u=a(x+y)^n f'(\eta) \ , \ v=a(x+y)^n g'(\eta)$$

$$w=-\sqrt{a\nu_f}\,(x+y)^{\frac{n-1}{2}} \left(\frac{n+1}{2}(f+g)+\frac{n-1}{2}\eta(f'+g')\right) \tag{7}$$

$$\theta(\eta)=\frac{T-T_\infty}{T_w-T_\infty} \ , \phi(\eta)=\frac{C-C_\infty}{C_\infty} \ , \eta=\sqrt{\frac{a}{\nu_f}}\,(x+y)^{\frac{n-1}{2}}z$$

Using equation (7), equation (1) satisfied perfectly also equation (2) to (6) reduce to

$$f''' + \left(\frac{n+1}{2}\right)(f+g)f'' - n(f'+g')f' + F_r f'^2 = 0 \quad (8)$$

$$g''' + \left(\frac{n+1}{2}\right)(f+g)g'' - n(f'+g')g' + F_r g'^2 = 0 \quad (9)$$

$$\frac{1}{Pr}\theta'' + \left(\frac{n+1}{2}\right)(f+g)\theta' + N_b\phi'\theta' + N_t\theta'^2 + E_c f''^2 = 0 \quad (10)$$

$$\phi'' + \left(\frac{n+1}{2}\right)S_c(f+g)\phi' + \frac{N_t}{N_b}\theta'' = 0 \quad (11)$$

$$\begin{aligned} &f(0) = g(0) = 0, f'(0) = 1, g'(0) = \lambda, \theta(0) \\ &= 1, N_b\phi'(0) + N_t\theta'(0) \\ &= 0, f'(\infty) \to 0, g'(\infty) \to 0, \theta(\infty) \to 0, \phi(\infty) \to 0 \end{aligned} \quad (12)$$

where, $\Pr = \nu_f / \alpha$ is Prandtl number, $N_b = \tau D_B C_\infty / \nu_f$ is element of Brownian motion,

$N_t = \tau D_T (T_w - T_\infty) / T_\infty \nu_f$ is the thermophoresis parameter, $\lambda = b/a$ is stretching rate ratio, and $Sc = \nu_f / D_B$ is Schmidt number. $F_r = \frac{c_b}{\rho_0\sqrt{k}}(x+y)$ is Forchheimer term and $E_c = \frac{u_w^2}{\rho_0 c_p (T_w - T_\infty)}$ is Eckert number. Skin friction factor and local Nusselt number, defined as follows,

$$C_{fx} = \frac{\tau_{zx}}{p_f u_w^2}, \; C_{fy} = \frac{\tau_{zy}}{p_f v_w^2}, \; Nu = \frac{(x+y)q_w}{k(T_w - T_\infty)} \quad (13)$$

where, τ_{zx} and τ_{zy} are tangential stresses acting on the wall andis thermal heat flux at wall, these are described as

$$\begin{aligned} &\tau_{zx} = \mu\left(\frac{\partial u}{\partial z} + \frac{\partial w}{\partial x}\right)_{z=0}, \quad \tau_{zy} = \mu\left(\frac{\partial v}{\partial z} + \frac{\partial w}{\partial y}\right)_{z=0}, \\ &q_w = -k\left(\frac{\partial T}{\partial z}\right)_{z=0} \end{aligned} \quad (14)$$

Applying equations (7) and (12) to the formula (14), we get

$$\begin{aligned} &Re_x^{\frac{1}{2}} C_{fx} = f^n(0), \; Re_y^{\frac{1}{2}} \lambda^{\frac{3}{2}} C_{fy} \\ &= g^n(0), \; Re_x^{\frac{-1}{2}} Nu = -\theta'(0) = Nur \end{aligned} \quad (15)$$

where, $Re_x = \frac{u_w(x+y)}{\nu_f}$ and $Re_x = \frac{v_w(x+y)}{\nu_f}$ are, respectively, the Reynolds numbers in x-y directions, respectively.

Velocity component at far field is considered as

$$w(x,y,\infty) = -\sqrt{a\nu_f (x+y)^{n-1}}\,\frac{n+1}{2}[f(\infty)+g(\infty)]$$

3.0 Methodology

By utilizing the RKF-NR approach, equations (8) – (11) is solved by applying the boundary condition (12). The constraints and equations are reduced into first order system

$$\begin{aligned} &f_1 = f, f_2 = f', f_3 = f'', f_4 = g, f_5 = g', \\ &f_6 = g'', f_7 = \theta, f_8 = \theta', f_9 = \phi, f_{10} = \phi' \end{aligned}$$

Thus we obtain

$$\begin{bmatrix} f_1' \\ f_2' \\ f_3' \\ f_4' \\ f_5' \\ f_6' \\ f_7' \\ f_8' \\ f_9' \\ f_{10}' \end{bmatrix} = \begin{bmatrix} f_2 \\ f_3 \\ -\left(\frac{n+1}{2}\right)(f_1+f_4)f_3 + n(f_2+f_5)f_2 - F_r f_2^2 \\ f_5 \\ f_6 \\ -\left(\frac{n+1}{2}\right)(f_1+f_4)f_6 + n(f_2+f_5)f_5 - F_r f_5^2 \\ f_8 \\ -Pr\left[\left(\frac{n+1}{2}\right)(f_1+f_4)f_8 + N_b f_8 f_{10} + N_t f_8^2 + E_c(f_3^2)\right] \\ f_{10} \\ -\left(\frac{n+1}{2}\right)Sc(f_1+f_4)f_{10} + \frac{N_t}{N_b}f_8' \end{bmatrix} \quad (17)$$

$$\begin{bmatrix} f_1(0) \\ f_2(0) \\ f_3(0) \\ f_4(0) \\ f_5(0) \\ f_6(0) \\ f_7(0) \\ f_8(0) \\ f_9(0) \\ f_{10}(0) \end{bmatrix} = \begin{bmatrix} 0 \\ 0 \\ u_1 \\ 0 \\ \lambda \\ u_2 \\ 1 \\ u_3 \\ u_4 \\ -\left(\frac{N_t}{N_b}\right)u_3 \end{bmatrix} \quad (18)$$

The equations (17) and (18) are solved by using the RKF-NR approach. We compared the result obtained with Khan *et al.*[14], Tables 1 and 2 give the good agreement.

Table 1. Comparison statement of second derivatives of f and g at x=0 for Fr=0=Ec

n	λ	$f''(0)$		$g''(0)$	
		Khan *et al.*,[14]	**Present Work**	**Khan *et al.*,[14]**	**Present Work**
1	0	-1	-1	0	0
	0.5	-1.224745	-1.22474311	-0.612372	-0.61237210
	1	-1.414214	-1.41421412	-1.414214	-1.41421400
3	0	-1.624356	-1.62435601	0	0
	0.5	-1.989422	-1.98942210	-0.994711	-0.99471101
	1	-2.297186	-2.29718601	-2.297186	-2.29718601

Table 2. Analysis of *Nur* in the absence of Forchheimer and viscous dissipation with Khan *et al.*[14]

n		Nt	Sc	Pr	Khan *et al.*,[14]	Present Work
3	0	0.1	10	7	2.4047	2.4048
		0.5			1.5793	1.5793
		0.7			1.2760	1.2760
	0.5	0.5	3	7	2.5883	2.5883
			5		2.3184	2.3184
			10		1.9342	1.9342
	1	0.5	10	7	2.2334	2.2334
				13	2.7055	2.7055
				25	3.2877	3.2877
				50	4.1151	4.1151
				100	5.3366	5.3366

4.0 Results and Discussions

The garnered outcomes are shown in Tables 1 and 2 which give the insights into the variations in the skin friction coefficients, non-dimensional components namely Prandtl number, Forchheimer, viscous dissipation, Schmidt number, Power law index, parameters of Brownian motion, thermophoresis, stretching rate ratio followed by temperature and concentration profiles.

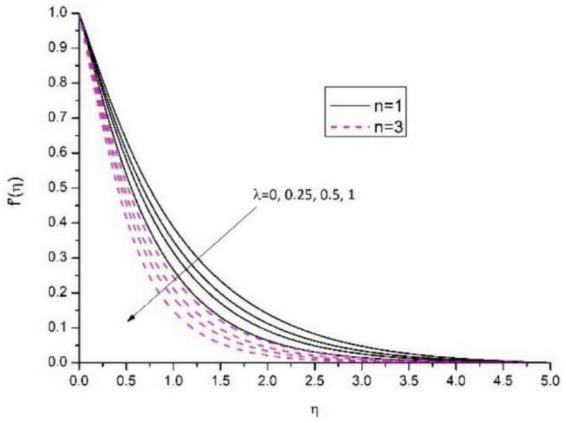


Figure 2. Influence of Stretching Rate Ratio on velocity

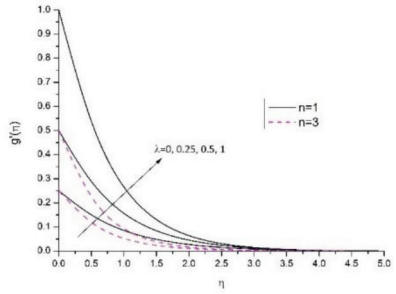


Figure 3. Influence of Stretching Rate Ratio on velocity .

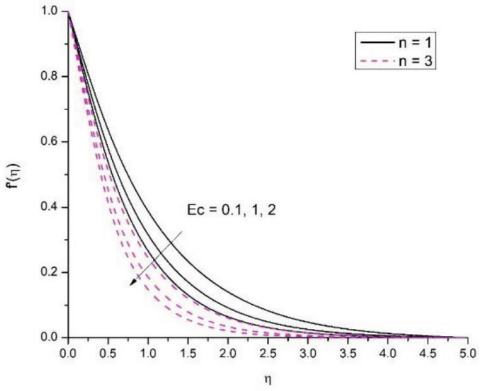


Figure 4. Influence of Eckert No. Ec on velocity

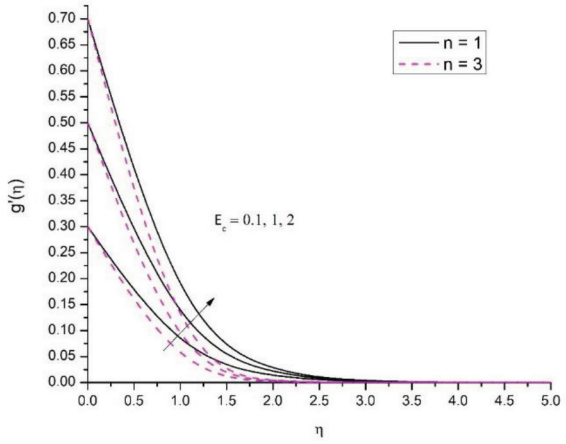


Figure 5. Influence of Eckert No. Ec on velocity

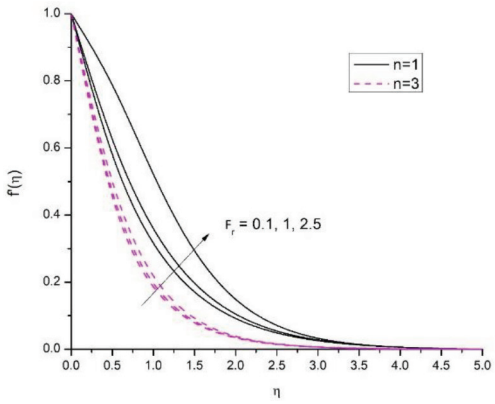


Figure 6. Influence of Forchheimer Fr on velocity

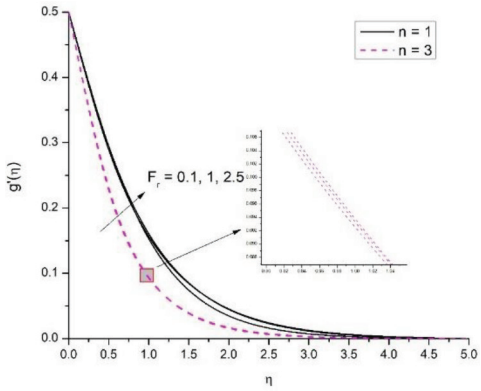


Figure 7. Influence of Forchheimer Fr on velocity

The numerical study has been conducted by varying the values of Pr, Nt, Nb, Fr, λ, n, Sc, Ec, shown in the graph. Figures 2-7 show the variations in the velocity profile for distinct range of stretching rate ratio (λ), Eckert number and Forchheimer along x-y directions. Elevating the values

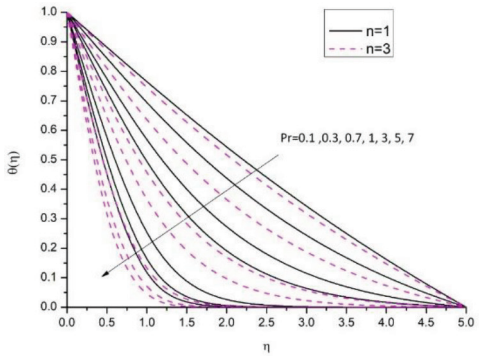


Figure 8. Influence of Prandtl No. Pr on temperature θ.

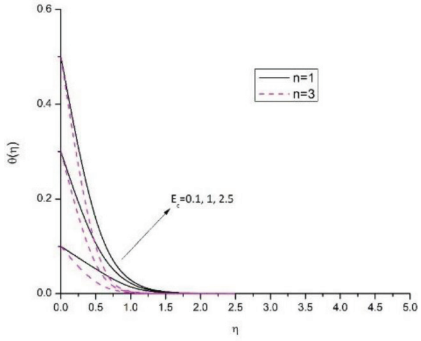


Figure 9. Influence of Eckert No. Ec on temperature θ.

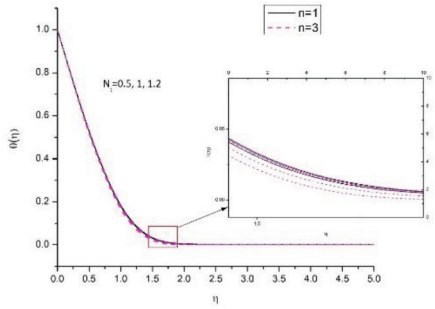


Figure 10. Influence of thermophoresis parameter Nt on temperature θ.

of λ, Ec, and Fr may result in a boost to the stretching rate by increasing the velocity along the y-axis and reduce the extending rate by decreasing the velocity along x – axis. The Figure 8 depicts the effect of Pr on the thermal boundary layer, a rise in pr corresponds with a reduction in the diffusivity of heat, which limits the ability of heat to travel further into the fluid. Consequently, thermal boundary region gets thinner as pr increases. We note that from the Figures 9-11, When the Eckert number, thermophoresis parameter and Schmidth number grows,

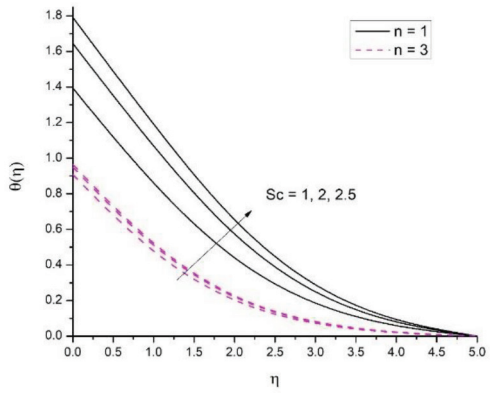


Figure 11. Influence of Schmidt no. Sc on temperature θ.

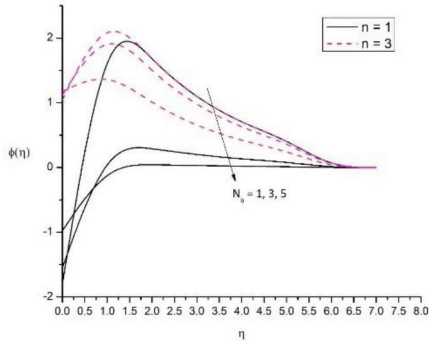


Figure 12. Influence of Brownian parameter Nb on volume fraction .

we note that the heat of the fluid also rises. This escalation in the thermophoretic force causes nanoparticles to migrate deeper within the surrounding fluid, consequently resulting in a thicker thermal boundary layer.

As the Brownian motion parameter increases, there is a corresponding decrease in the volume fraction of particles within the fluid. This phenomenon can be attributed to the heightened Brownian motion causing particles to diffuse more rapidly throughout the fluid, leading to a dispersion that reduces the overall volume fraction of particles in the system is observed in Figure 12. The variations of Sc on temperature are shown in Figure 11 to understand the thermal conductivity of the boundary layer changes as the Schmidt number (Sc) rises. Higher Sc values signify greater molecular motion within the fluid, resulting in subsequent increase in fluid temperature.

5.0 Conclusions

The study investigates the impact of Forchheimer Drag and viscous dissipation on nanofluid past a 3D nonlinear extending sheet, considering the existence of Forchheimer and viscous dissipation. Utilizing similarity transformation, the governing equations are transformed and solved utilizing the RKF-NR approach. Results are obtained for various parameters including velocity, temperature, nanoparticle volume fraction, Prandtl number, Eckert number, and stretching rate. Here are the main findings of this research:

- Enhanced viscous dissipation increases temperature within the thermal boundary layer, resulting in its expansion.
- Elevated non-dimensional components such as the Eckert number, Thermophoresis, and Schmidt number correspond to an increase in temperature.
- Increasing the Prandtl number and Brownian parameter leads to a reduction in both temperature and nanoparticle volume fraction, respectively.
- A larger Brownian parameter indicates a less uniform distribution of nanoparticles.
- With an increasing thermophoresis parameter, temperature at which heat transfers to the surface is quantified by the local Nusselt number which decreases.
- Increasing the stretching rate results in amplified velocity along the y-direction and diminished velocity along the x-direction.
- Forchheimer's equation and viscous dissipation effects are vital in hydraulic fracturing in oil and gas extraction, oil and gas pipeline transportation, fuel injection systems in combustion engines.

6.0 Acknowledgement

The authors are grateful to KSSEM, JSSATE and MSRIT for supporting collaboration research work.

7.0 References

1. Masood S, Farooq M, Ahmad S, Anjum A, Mir NA. Investigation of viscous dissipation in the nanofluid flow with a Forchheimer porous medium: Modern transportation of heat and mass. Eur Phys J Plus. 2019; 134:178. https://doi.org/10.1140/epjp/i2019-12519-0
2. Rasool G, Shafiq A, Alqarni MS, Wakif A, Khan I, Bhutta MS. Numerical scrutinization of Darcy-Forchheimer relation in convective magnetohydrodynamic nanofluid flow bounded by nonlinear stretching surface in the perspective of heat and mass transfer. Micromachines. 2021; 12:374. https://doi.org/10.3390/mi12040374

3. Abderrahmane A, Jamshed W, Abed AM, Smaisim GF, Guedri K, Devi SSU, *et al*. Heat and mass transfer analysis of non-Newtonian power-law nanofluid confined within annulus enclosure using Darcy-Brinkman-Forchheimer model. Case Stud Therm Eng. 2022; 40:102569. https://doi.org/10.1016/j.csite.2022.102569
4. Dada MS, Adefolaju FH. Dissipation, MHD and radiation effects on an unsteady convective heat and mass transfer in a Darcy-Forcheimer porous medium. J Math Res. 2012; 4:110. https://doi.org/10.5539/jmr.v4n2p110
5. Bhatti MM, Zeeshan A, Ellahi R, Shit GC. Mathematical modeling of heat and mass transfer effects on MHD peristaltic propulsion of two-phase flow through a Darcy-Brinkman-Forchheimer porous medium. Adv Powder Technol. 2018; 29:1189-97. https://doi.org/10.1016/j.apt.2018.02.010
6. Dinesh PA, Kumar BR, Babu RS. Combined effects of internal heat generation and viscous dissipation for double diffusive with Forchheimer fluid model. Sixth International Conference on Porous Media and its Applications in Science, Engineering and Industry; 2016.
7. Dinesh PA, Nalinakshi N, Chandrashekhar DV. Effects of internal heat generation and variable fluid properties on mixed convection past a vertical heated plate. Fluid Dynam Mater Process. 2014; 10:465-90. https://doi.org/10.3970/fdmp.2014.010.465
8. Bandaru M. double diffusive convection of a rotating fluid over a vertical plate embedded in Darcy-Forchheimer porous medium with non-uniform heat sources. Internat J Emerg Trends Eng Develop. 2013; 2:415-32. https://www.researchgate.net/publication/269995377
9. Alrihieli H, Alrehili M, Megahed AM. Radiative MHD nanofluid flow due to a linearly stretching sheet with convective heating and viscous dissipation. Mathematics. 2022; 10:4743. https://doi.org/10.3390/math10244743
10. Sheikholeslami M, Abelman S, Ganji DD. Numerical simulation of MHD nanofluid flow and heat transfer considering viscous dissipation. Int J Heat Mass Transf. 2014; 79:212-22. https://doi.org/10.1016/j.ijheatmasstransfer.2014.08.004
11. Ramesh NL, Dinesh PA, Brijesh, Shilpa BV. Effect of diffusion-thermal on mixed convective Casson fluid flow in a porous channel. J Mines Met Fuels. 2023:1526-36. https://doi.org/10.18311/jmmf/2023/35811
12. Kavitha S, Nalinakshi N, Dinesh PA, Brijesh. Analysis of Forchheimer effect for double diffusive convection with Dusty Fluids and MHD. J Mines Met Fuels. 2023:2289-99. https://doi.org/10.18311/jmmf/2023/36331
13. Roopa KR, Dinesh PA, Yadav S, Vinay CV, Subrahmanyam C. Comparative heat transfer analysis of Fe3O4/Graphene-water hybrid nanofluid in unsteady hydrodynamic Lapwood-Brinkmann Forchheimer medium over a curved elongating region. Int J Ambient Energy. 2024; 45:2304714. https://doi.org/10.1080/01430750.2024.2304714
14. Khan JA, Mustafa M, Hayat T, Alsaedi A. Three-dimensional flow of nanofluid over a non-linearly stretching sheet: An application to solar energy. Int J Heat Mass Transf. 2015; 86:158-64. https://doi.org/10.1016/j.ijheatmasstransfer.2015.02.078
15. Raju CSK, Sandeep N. Unsteady three-dimensional flow of Casson-Carreau fluids past a stretching surface. Alex Eng J. 2016; 55:1115-26. https://doi.org/10.1016/j.aej.2016.03.023
16. Buongiorno J. Convective transport in nanofluids. J Heat Transfer. 2005; 128:240-50. https://doi.org/10.1115/1.2150834
17. Riaz A, Zeeshan A, Bhatti MM, Ellahi R. Peristaltic propulsion of Jeffrey nano-liquid and heat transfer through a symmetrical duct with moving walls in a porous medium. Phys A: Stat Mech Appl. 2020; 545:123788. https://doi.org/10.1016/j.physa.2019.123788
18. Necib N, Benkhedda M, Tayebi T, Boufendi T. Three-dimensional mixed convection and entropy generation of binary and ternary hybrid nanofluids flow inside a porous media-filled horizontal annular duct under magnetic field. J Therm Anal Calorim. 2024; 149:813-38. https://doi.org/10.1007/s10973-023-12717-w

Nomenclature

x, y, z	Coordinate system in cartesian geometry
u, v, w	Velocity
u_w, v_w	Velocity of the stretched sheet.
T_f	Fluid Temperature
T_w	Temperature at the wall
T_∞	Ambient temperature
C	Volume fraction of local nanoparticles
C_∞	Volume fraction of ambient nanoparticles
a, b, n	Constants
Pr	Prandtl number
Sc	Schmidt number
f, g	Non-Dimensional velocity factor
k	Thermal Conductivity
Nu	Nusselt number
Nur	Decreased Nusselt number
q_w	Wall heat flux
D_B	The diffusion coefficient of Brownian matter
D_T	Thermophoresis Diffusion Coefficient
Nt	Thermophoresis parameter
$Re_x; Re_y$	Local Reynolds numbers in x- y axes.
$C_{fx}; C_{fy}$	Skin friction factors.
Nb	Brownian motion parameter
τ	Ratio of the nanoparticle's effective heat capacity to that of the base fluid
V_f	Fluid's kinematic viscosity

α	Thermal diffusivity
η	Similarity variable
λ	Ratio of the stretching rates
μ_f	Dynamic viscosity
ν_f	Fluid density
ϕ	Volume fraction of dimensionless nanoparticles
τ_{zx}, τ_{zy}	Tangential stress
θ	Dimensionless temperature